The dynamics of spawning acts by a semelparous fish and its associated energetic costs

Cédric TENTELIER[1,2,a], Colin BOUCHARD[1,2,3,b], Anaïs BERNARDIN[1], Amandine TAUZIN[1], Jean-Christophe AYMES[1,2,c], Frédéric LANGE[1,2,d], Charlotte RECAPET[1,2,e], Jacques RIVES[1,2,f]

[1] Universite de Pau et des Pays de l'Adour, E2S UPPA, INRAE, ECOBIOP, Saint-Pée-sur-Nivelle, France

[2] Pôle Gestion des Migrateurs Amphihalins dans leur Environnement, OFB, INRAE, AGROCAMPUS OUEST, UNIV PAU & PAYS ADOUR/E2S UPPA

[3] Tour du Valat, Research Institute for the Conservation of Mediterranean Wetlands, Arles, France

[a] ORCID: 0000-0003-2178-4900
[b] ORCID: 0000-0003-0845-9492
[c] ORCID: 0000-0002-1181-3010
[d] ORCID: 0000-0001-8561-1879
[e] ORCID: 0000-0001-5414-8412
[f] ORCID: 0000-0001-6074-3488

Corresponding author: Cédric TENTELIER,
Universite de Pau et des Pays de l'Adour
Collège STEE – Campus de la côte basque
1 allée du parc Montaury
64 600 Anglet, France.
cedric.tentelier@univ-pau.fr

Abstract

1. During the reproductive season, animals have to manage both their energetic budget and gamete stock. In particular, for semelparous capital breeders with determinate fecundity and no parental care other than gametic investment, the depletion of energetic stock must match the depletion of gametic stock, so that individuals get exhausted just after their last egg is laid and fertilized. Although these budgets are managed continuously, monitoring the dynamics of mating acts and energy expenditure at a fine temporal scale in the wild is challenging.

2. This study aimed to quantify the individual dynamics of spawning acts and the concomitant energy expenditure of female Allis shad (*Alosa alosa*) throughout their mating season.

3. Using eight individual-borne accelerometers for one month, we collected tri-axial acceleration, temperature, and pressure data that we analysed to i) detect the timing of spawning acts, ii) estimate energy expenditure from tail beat frequency and water temperature, and iii) monitor changes in body roundness from the position of the dorsally-mounted tag relative to the vertical plane.

4. Female shad had a higher probability to spawn during warmer nights, and their spawning acts were synchronized (both individually and inter-individually) within each active night. They experienced warmer temperature, remained deeper, swan more slowly and spent less energy during daytime than night time. Over one month of spawning, they performed on average 15.75 spawning acts, spent on average 6 277 kJ and died with a significant portion of residual oocytes. The acceleration-based indicator of body roundness was correlated to condition coefficient measured at capture, and globally decreased through the spawning season, although the indicator was noisy and was not correlated to changes in estimated energy expenditure.

5. Despite significant individual variability, our results indicate that female shad exhausted their energetic stock faster than their egg stock. Water warming will increase the rate of energy expenditure, which might increase the risk that shad die with a large stock of unspent eggs. Although perfectible, the three complimentary analyses of acceleration data are promising for *in situ* monitoring of energy expenditure related to specific behaviour.

Keywords

Accelerometer, biologging, clupeid, egg retention, energy budget, reproductive effort, semelparity, temperature, slimming.

Introduction

The energy acquired by living organisms is allocated to survival and reproduction, and natural selection is expected to favour optimal allocation, resulting in life-histories that maximize Darwinian fitness in the environment where evolution occurs (Pianka 1976; Stearns 1992; Roff 1993). When adult survival is low compared to juvenile survival, extreme reproductive effort (in gametogenesis, mating behaviour and parental care) can be selected and semelparity may arise, in which individuals die after their first and only breeding season. Semelparity is often accompanied with capital breeding, so that reproduction relies on energy reserves constituted before the breeding season (Bonnet et al. 1998). Although semelparity is sometimes quoted as "big bang reproduction", its broad definition encompasses cases where individuals breed in several bouts within a breeding season (Kirkendall and Stenseth 1985; Hughes 2017). Furthermore, in species with no other parental care than gametic investment, the optimal allocation should result in individuals dying just after their last progeny is produced, and deviation from optimality consists in individuals either surviving after their last egg is laid and fertilized, or dying of exhaustion while still bearing unlaid eggs (Heimpel and Rosenheim 1998). Hence, the schedule of breeding events and the dynamics of energy expenditure during the breeding season, which may be pronounced in semelparous capital breeders, is a crucial aspect of reproductive strategy.

Beside energy expenditure, the temporal distribution of breeding events within a season may be linked to ecological, pheromonal or behavioural cues that synchronize breeding activity (Gochfeld 1980; Ims 1990; Fürtbauer et al. 2011). Here, internal and external stimulations probably interact, with the hormone-driven reproductive cycle and energetic condition determining whether an individual is ready to breed at a given time, and social or ecological factors triggering the actual breeding behaviour (Jovani and Grimm 2008; Koizumi and Shimatani 2016). At the ultimate level, reproductive synchrony affects intraspecific

87 competition for resources (including mates; Emlen and Oring 1977) and the risk of predation
88 on breeders or their offspring (Ims 1990).

89 Tracking the schedule of breeding events and the dynamics of energy expenditure of
90 breeding individuals in the wild is technically challenging. The timing of breeding events along
91 the breeding season requires thorough observation of repeatedly detectable individuals, for
92 example through video recording of highly sedentary individuals (e.g. Borgia 1985). Energy
93 expenditure has been monitored at the population level, by quantifying energy reserves on
94 different individuals sampled at different stages of the breeding season (e.g. Hendry and Berg
95 1999). In some cases, the same individuals were captured at the beginning and at the end of the
96 breeding season, and the energy expenditure quantified with difference in mass (Anderson and
97 Fedak 1985; Rands et al. 2006), body composition (Hendry and Beall 2004; Casas et al. 2005),
98 or concentration of plasma metabolites (Gauthey et al. 2015). Likewise, in terrestrial animals,
99 the turnover of ^{18}O and ^{2}H from doubly labelled water quantifies the average field metabolic
100 rate at the individual level between two sampling occasions (Nagy et al. 1999). All these
101 methods give a good idea of the total energy expenditure over the whole breeding season but
102 often lack the temporal resolution to document the longitudinal dynamics of energy expenditure
103 all along the breeding season.

104 With the advent of bio-logging, the temporal resolution of individual data collected in
105 the field has tremendously increased. Among bio-loggers, accelerometers, often coupled with
106 other sensors such as thermometers, have been increasingly used, and advances in their
107 energetic efficiency now allows to record high-frequency data for weeks or months, making
108 them valuable tools for longitudinal studies of breeding behaviour in many organisms. In this
109 context, acceleration data can quantify both the overall movement of tagged individuals (overall
110 dynamic body acceleration), which can be translated in energy through laboratory calibration
111 (Wilson et al. 2006; Groscolas et al. 2010; Collins et al. 2016; Hicks et al. 2017; Wilson et al.

2019), and the number and temporal distribution of key behaviours such as mating events, if these produce a typical acceleration pattern (Brown et al. 2013).

This study aimed at describing the activity and change in body condition of female Allis shad (*Alosa alosa* L. 1758) throughout their spawning season. Allis shad is a semelparous anadromous clupeid, a capital breeder with determinate fecundity (Baglinière et al. 2003). It is also a major halieutic resource in the Atlantic coast of southern Europe, and the size of most of its populations has plummeted since the beginning of the 21st century. Its economical and conservation value and its spawning behaviour are such that the timing of its reproduction is very well documented at the population level. The spawning act consists of at least one male and one female swimming side by side during five to ten seconds while describing three to five circles of one meter in diameter and beating the water surface vigorously with their tail (Baglinière and Elie 2000). The typical splashing noise (35 dB at one meter) can be heard and recorded from the river bank, and the number of splashes recorded during the spawning season is often used as an indicator of the number of spawners in a population (Chanseau et al. 2004). Despite the wealth of data on the timing of spawning acts across the season and within nights at the population level, no reliable data exist at the individual level (but see Acolas et al. 2004 for a previous attempt), which is the appropriate level to eventually address the fitness associated to behavioural strategies.

Using accelerometers, we investigated three main aspects and tested specific predictions:

1) We described the individual schedule of spawning events, which were identified using a characteristic acceleration pattern. We tested whether the probability of spawning increased solely with water temperature (Paumier et al. 2019) or was also affected by internal and social factors. In particular, as oocytes seem to mature in five to seven batches (Cassou-Leins and Cassou-Leins 1981), we expected shad to perform five to seven spawning acts separated by a consistent time lapse corresponding to the

maturation time of each batch. Moreover, given the aggregative behaviour of shad, which shoal even during the spawning season (Baglinière and Elie 2000), we tested whether different females synchronize their spawning acts within a night.

2) We quantified global activity as tail beat frequency, and converted it to energy expenditure through an energetic model including water temperature. This was used to identify variability in energy expenditure between periods of the spawning season and to test the effect of energy management on the risk of dying with unlaid eggs. In particular, we tested the predictions that shad were more active and spent more energy during the night than during the day, and that the individuals that better managed their energy expenditure (higher night time energy expenditure and lower daytime energy expenditure) died with fewer residual eggs.

3) We tested the possibility to use the angle between the dorsally-mounted accelerometer and the vertical plane as an indicator of body roundness of the fish. This novel method would allow monitoring the slimming process through the spawning season, and relating it to periods of high energy expenditure. We predict that if the angle of the accelerometer is a reliable indicator of fish condition, it should a) be correlated to the individual coefficient of condition measured at the beginning and the end of the spawning season, b) decrease across the spawning season, as the fish slims, c) decrease proportionally to mass loss, d) decrease more rapidly during periods of high energy expenditure.

Methods

Characteristics of the species studied

Allis shad (*Alosa alosa* L.) is an anadromous clupeid fish distributed along the Atlantic coast of Europe, from Portugal to the British Isles, with the main populations dwelling in the French rivers Garonne, Dordogne and Loire (Baglinière and Elie 2000). Across its distribution, Allis shad is considered as a semelparous species, although spawning marks on scales suggest that a very small proportion of individuals may spawn on two consecutive years (Mennesson-Boisneau and Boisneau 1990; Taverny 1991). After having spent a few months in freshwater as juveniles and four to six years at sea, shad undertake freshwater upstream migration during which they fast, thus qualifying as capital breeders. Gonad maturation occurring during migration leads females to bear between 13 000 and 576 000 eggs, reaching an average gonad mass of 221 g and a gonad / somatic mass ratio of 15% on spawning grounds (Cassou-Leins and Cassou-Leins 1981; Taverny 1991). Spawning typically occurs at night in a 0.3 to 3 metre-deep glide. As mentioned above, the spawning act consists of rapid circular swimming and vigorous tail beating for five to ten seconds, and should produce an easily detectable acceleration pattern. Although very few data are available, the number of splashes recorded upstream from dams where migrating shad were counted suggest that females perform on average five to twelve spawning acts during the season (Fatin and Dartiguelongue 1996; Acolas et al. 2006). Moreover, based on the dynamics of ovary index and oocyte diameter measured on individual caught and dissected across the season, Cassou-Leins & Cassou-Leins (1981) postulated that shad mature their eggs in five to seven batches.

The spawning season spans from early-May to late July, but dead individuals can be collected downstream from spawning ground as soon as late May. The number of splashes heard on spawning ground increases with increasing water temperature (Baglinière and Elie 2000; Paumier et al. 2019), but this could be due to either more individuals being sexually active

or individuals to be more active at higher temperature. Within a night, the temporal distribution of splashes in large populations typically follows a Gaussian distribution centred on 2 AM and spanning from 10 PM to 6 AM (Cassou-Leins and Cassou-Leins 1981).

Shad being capital breeders, samples of different individuals caught at different times during the migration and reproduction have shown dramatic changes in somatic mass and tissue composition (Cassou-Leins and Cassou-Leins 1981; Bengen 1992), but no longitudinal data exist at the individual level.

Fieldwork

We conducted this study in spring 2017 and 2018 in the Nivelle, a 39 km long coastal river situated in the Northern Basque Country, France, and draining a 238 km² basin. The downstream limit of the study zone was the impassable Uxondoa weir, situated 12 km upstream from the river mouth (43°21'40.64"N, 1°35'13.99"W), and equipped with a vertical slot fishway and a trap where a yearly average of 230 (min = 26; max = 688) migrating shad have been counted since 1996, with less than 30 individuals per year since 2015. Five kilometres upstream from Uxondoa stands another impassable weir equipped with a fishway and a trap, where shad have almost never been captured.

The Uxondoa fish trap was controlled daily throughout spring (ECP 2018). Nine female shad were captured and tagged in 2017, and 15 in 2018. All experimental procedures comply with French and European legislation, and were approved by the legal representative (prefectural decree #64-2017-04-25-004) and the ethical committee for birds and fishes in the French region Nouvelle Aquitaine (authorization #2016020116037869). The tagging procedure was quite similar to Breine (2017) for twaite shad (*Alosa fallax*). We anesthetized each individual in a bath of 15 mg/L benzocaine diluted in river water before weighing it, measure its fork length, gently press the abdomen to check the absence of sperm emission, and finally

208 tag it with a radio transmitter emitting at a unique frequency (F2020, ATS, Isanti, MN, USA)
209 and a three-dimensional accelerometer (WACU, Atesys-Montoux, Huguenau, France). For
210 tagging, each fish was kept in a 20 L tank filled with anaesthetic solution (Fig. 1.A). A water
211 pump placed in the fish's mouth and a stone bubbler in the bath ensured a good circulation of
212 aerated water during the tagging procedure. Adjustable plastic plates covered with foam were
213 placed vertically against both flanks to maintain the fish in an upright position, with only its
214 back being above water surface. The radio transmitter and the accelerometer were cleaned with
215 a povidone iodine solution (Betadine®) and dried with surgical cotton. The two Teflon-coated
216 metallic wires of the radio transmitter were inserted 1 cm under the dorsal fin through sterile
217 hollow needles. The hollow needles were then removed, and the metallic wires were passed
218 through holes drilled in the accelerometer's lug, secured with plastic eyelets and aluminium
219 sleeves, and the extra length was cut. The radio transmitter and the accelerometer weighed 8.6
220 g and 9 g, respectively, so the weight was balanced on both sides of the fish. After tagging, each
221 fish was placed in a 50 L box filled with river water, and released upstream from the weir upon
222 waking.

223 From its release at Uxondoa weir until its death at the end of the spawning season, each
224 tagged shad was localized twice a day using a mobile receiver (R2100, ATS, Isanti, MN, USA)
225 and a loop antenna, in order to check whether it was still alive and to obtain its position. The
226 radio transmitters were set to double their pulsing rate after 8 h of total immobility. Within two
227 days after double pulse was detected, the dead fish and the tags were recovered by snorkelling,
228 and the whole fish and its ovaries were immediately weighed.

229

230 ## Processing acceleration data

231 The loggers used in this study recorded acceleration between -8 g and +8 g (1 g = 9.81
232 $m.s^{-2}$) in each of the three dimensions at an average frequency of 50 logs per second. Every

second, they also recorded the temperature, pressure, date, time and exact number of acceleration logs within the past second. Both dynamic and static (gravitational) acceleration were used to estimate three types of variables: body roundness through the angle of the accelerometer with the vertical plane, tail beat frequency and occurrence of spawning acts.

The static, gravitational, component on each axis *i* (*x, y* and *z*) was extracted from the raw signal at each time *t* by replacing each data point $\overrightarrow{A_{i,t}}$ by the average of the points within a window of width *w* centred on *t*, so that:

$$\overrightarrow{SA_{i,t}} = \frac{1}{w} \sum_{j=t-\frac{w}{2}}^{j=t+\frac{w}{2}} \overrightarrow{A_{i,j}}$$

Unlike what is usually done (Brown et al. 2013), these data were not used to assess the posture of the fish, as no known behaviour in shad involves change of posture. Instead, we hypothesized that it may reflect the shape of the fish. Indeed, since the accelerometer was pinned on the dorsal part of the fish's flank, the angle θ between the *x*-axis of the tag and the vertical plane may be linked to the roundness of the fish, a proxy of its energetic reserves. This angle could be computed at any data point of static acceleration, as $\theta_t = cos^{-1}(\overrightarrow{SA_{x,t}})$, where θ_t is the angle at time *t* and $\overrightarrow{SA_{x,t}}$ is the static acceleration computed on the *x*-axis at time *t* (Fig. 1.B). To track change in body roundness through the season, θ was estimated for each fish from $\overrightarrow{SA_{x,t}}$ computed over *w*=180 000 points (*i.e.* 1 h at a 50Hz sampling frequency) every eight hours (6AM, 2PM, 10PM), from its release until its death.

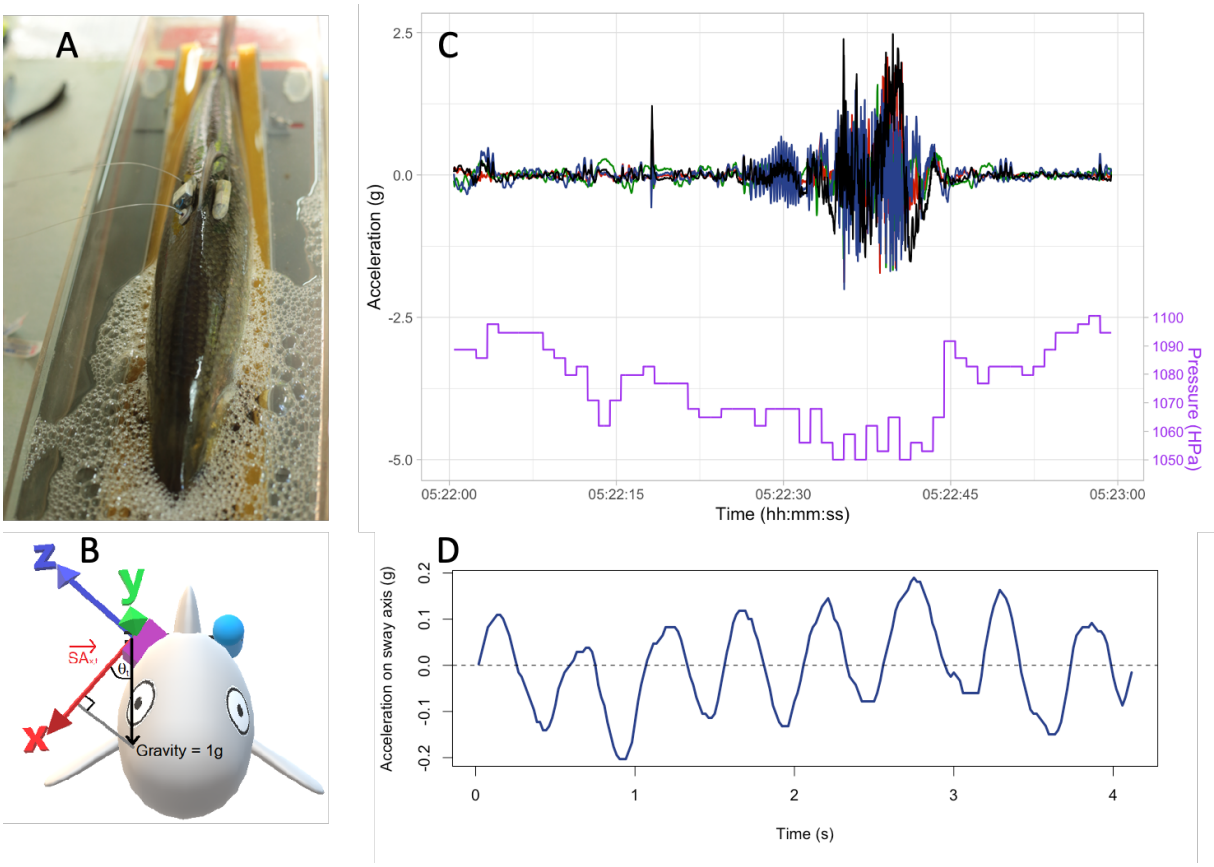

Figure 1. A. Allis shad were tagged under anaesthesia with a radio transmitter on the left flank and an accelerometer on the right flank. The accelerometer continuously recorded acceleration on three axes. B. The static component of acceleration recorded on the x-axis at time t, $\overrightarrow{SA_{x,t}}$, corresponds to the orthogonal projection of gravity, which is vertical by definition, on this axis. Hence, the angle θ between the x-axis and the vertical plane can be computed for any time t as $\theta_t = cos^{-1}(\overrightarrow{SA_{x,t}})$. C. The dynamic component of acceleration (here smoothed with a 31-point wide median filter) can be used to detect spawning acts, characterized by increased acceleration on both x (red), y (green) and y (blue) axes, resulting in a peak in the norm of the 3-dimensional acceleration vector (black), and accompanied by a decrease in hydrostatic pressure (purple). D. After correction for the θ angle, the z-axis corresponds to the sway axis of the fish, and its dynamic component (here smoothed with a 5-point wide median filter) can be used to compute tail beat frequency (TBF) as the number of zero-crossings per unit of time.

266 The dynamic component of acceleration was computed at every time point on each
267 dimension i ($\overrightarrow{DA_{i,t}}$) as the raw signal minus the static acceleration computed over w=250 points
268 (= 5 s at 50 Hz). This was used to count the number of spawning events performed by each
269 tagged shad. To do this, the acceleration pattern typical of spawning act was first described in
270 a controlled experiment and then searched in the field-collected data. To characterize the typical
271 pattern associated with spawning act, a male (420 mm, 855 g) and a female (460 mm, 1140 g)
272 shad were captured at Uxondoa trap, tagged as described above, and observed for one month
273 (June 2016) in a basin (400 m², 0.6 m water depth) at the INRAE experimental facilities in St
274 Pée sur Nivelle (ECP 2018). Eight spawning acts were recorded on video or audio, which could
275 be compared with acceleration data. The typical pattern of acceleration associated to the
276 spawning act was a rise in the norm of the 3D acceleration vector, which stayed above 3 g for
277 at least 3 seconds, mainly driven by acceleration on the z-axis corresponding to TBF reaching
278 up to 15 beats per second. (Fig. 1.C). A decrease of hydrostatic pressure was typically
279 associated to this pattern, due to the fish reaching the water surface during the spawning act.
280 These criteria for identification of spawning acts were robust, as they were always detected
281 when spawning was visually observed (no false negative) and never observed when spawning
282 was not visually observed (no false positive). These criteria were implemented in an algorithm
283 to scan the accelerograms collected in the field in 2017. This automated identification was
284 validated by visual comparison of accelerogram sequences automatically identified in 2017
285 with sequences of eight acknowledged spawning acts recorded in 2016.

286 The dynamic acceleration was also used to quantify the activity of the fish through Tail
287 Beat Frequency (TBF), computed as the number of zero-crossings per second of $\overrightarrow{RDA_{z,t}}$ on
288 which a median filter (window width = 5 points) was applied for noise reduction (Fig. 1.D).
289 Acceleration on the sway axis is commonly used to measure TBF on fishes of different species
290 and sizes (Kawabe et al. 2003; Tsuda et al. 2006; Broell and Taggart 2015; Brownscombe et al.

2018), and preliminary data on the two captive individuals mentioned above showed that our acceleration-based measurement of TBF corresponded to the visual measurement. TBF can be computed at every instant, but for further analysis we used average computed for every minute.

We estimated the energy consumption for every minute of each individual's reproductive season, using its tail beat frequency (computed as described above), the temperature recorded by the individual logger, and equations derived from the data of Leonard et al. (1999) and Castro-Santos & Letcher (2010) on American shad, *Alosa sapidissima*. Leonard et al. (1999) measured oxygen consumption and tail beat frequency of 18 American shad in a swimming respirometer with water temperature varying between 13°C and 24°C. On their data, we fitted a linear mixed model (lmer function in lme4 package; Bates et al. 2014) with individual random intercept and fixed effects of temperature and TBF, on log-transformed oxygen demand (MO_2, in mmol $O_2.kg^{-1}.h^{-1}$). Then, assuming that 0.4352 kJ of somatic energy are burnt per mmol O_2 (Brett and Groves 1979), we used the three parameters of the mixed model (average intercept = 1.0064, slope of temperature = 0.0531, and slope of TBF = 0.2380) to compute the amount of energy $E_{i,t}$ (in kJ) consumed by each fish i for each minute t of its spawning period, from its body mass $M_{i,t}$ (in kg), the average temperature recorded by its logger during that minute $T_{i,t}$ (in °C), and its average tail beat frequency during that minute $TBF_{i,t}$ (in beat per second):

$$E_{i,t} = \frac{1}{60} \times 0.4352 \times M_{i,t} \times e^{1.0064+0.0531\times T_{i,t}+0.2380\times TBF_{i,t}} \quad \text{(Equation 1)}$$

Since energy consumption continually reduces fish mass, we iteratively modelled fish mass and energy expenditure at each minute of the spawning season. For this, we assumed that shad get 69% of their energy from lipids and 31% from proteins to fuel their metabolism (Leonard & McCormick, 1999), and that one gram of fat yields 39.54 kJ, against 23.64 kJ per gram of protein (Craig et al. 1978), so fish mass at the tth minute was:

$$M_{i,t} = M_{i,t-1} - \frac{E_{i,t}}{0.69\times 39.54+0.31\times 23.64}.10^{-3} \quad \text{(Equation 2)}$$

316 Finally, the exact timing of each individual's death was detected as a clear change in the
317 acceleration signal, where the gravitational component indicated that the fish switched from
318 upright posture to lying on its side or upside down, and the only dynamic component left was
319 the tenuous jiggling due to water flowing over the tag.

320 Beside acceleration, the pressure data given by the tags was processed to translate it to
321 depth by computing hydrostatic pressure (1hPa.cm^{-1}) as the difference of pressure recorded
322 every second by each tag and the atmospheric pressure recorded every 20 minutes by a
323 meteorological station situated at the INRAE facilities, less than one kilometre from the
324 spawning ground.

325

326 ## Statistical analysis

327 All analyses were performed on R (R Development Core Team 2008). A zero-inflated
328 mixed regression (package glmmTMB; Brooks et al. 2017) was used to test the effect of
329 temperature on the number of spawning acts performed by each individual on each night. The
330 Binomial component of the model informed on the effect of temperature on the probability to
331 perform any spawning act, while the Poisson component tested the effect of temperature on the
332 number of spawning acts. Individual was used as a random effect on both components. To test
333 whether females spawning in the same night synchronized their spawning acts with each other,
334 we performed 10 000 permutations of the hour of spawning acts recorded along all nights, and
335 compared the median of the delay to the nearest spawning act for actual data and for simulated
336 data. Because our aim was not to test the synchrony between acts performed by the same female,
337 only the first act performed by each female on a given night was considered in this analysis.

338 As mentioned above, TBF was computed for every minute of each individual's
339 spawning season, to track its energy expenditure. As an indicator of fish activity, average TBF
340 was also aggregated over eight-hour time windows corresponding to three periods of the day:

morning (6AM-2PM), afternoon (2PM-10PM) and night (10PM-6AM). The limits of the night period correspond to the earliest and latest hour of spawning activity classically recorded on spawning grounds (Cassou-Leins and Cassou-Leins 1981). To test whether shad adopted a different behaviour at different periods of the day, linear mixed models with individual random intercept and period of the day as a fixed effect were fitted to TBF, temperature and depth. For TBF, we also added a binary covariate indicating whether the fish had been tagged for more or less than three days, to test whether recent tagging increased activity (as observed in Atlantic salmon by Føre et al. 2020). All mixed models were fitted using the package lme4 for R (Bates et al. 2014), significance of fixed effects was tested using the likelihood ratio test (LRT χ^2) between the model including the fixed effect and the nested model excluding it. Marginal and conditional R^2 (R^2_m and R^2_c), indicating the proportion of variance explained by the fixed effects and by the whole model, respectively, where computed using R package MuMIn (Barton 2009).

To our knowledge, static acceleration has never been used to assess changes in animal body roundness. As mentioned in the introduction, we tested four predictions resulting from the hypothesis that the angle θ between the x-axis of an individual's accelerometer and the vertical plane was an indicator of body roundness. First, we fitted a Pearson correlation between Fulton condition coefficient (100*mass (in grams)/length (in centimetres)^3) and θ, both measured at the initial capture and at death. Second, a linear mixed model, with individual random intercept and slope was used to test whether θ decreased with time since individual release. Depth was added in this model, to account for the possibly positive effect of swim bladder inflation (hence negative effect of depth) on body roundness. Third, to test if change in θ over the breeding season was proportional to change in condition, a correlation was performed between the differences in θ and in Fulton condition coefficient from release to death. Finally, to test whether the decrease in θ could be linked to temperature, activity, energy expenditure or the moment of the days, we fitted linear mixed models with the difference in θ between the first

and the last hour of each 8-hour period and an individual random intercept. Four models were tested, 1) the null model with only random intercept, 2) a model with average temperature and TBF during the 8-hour period as fixed effects, 3) a model with cumulated energy expenditure during the 8-hour period as a fixed effect, and 4) a model with the moment of the period (morning, afternoon, night) as a fixed effect. To compare mixed models corresponding to alternative hypotheses, we used Akaike Information Criterion corrected for small sample bias (AICc) on R package MuMIn (Barton 2009).

The R code for statistical analysis and the data sets on which they were performed are available in the institutional data repository of the INRAE (French National Institute for Agriculture Food and Environment): https://doi.org/10.15454/NTFYCC.

Results

The nine female shad tagged in 2017 survived between 20 and 37 days (mean=26 days), and all tags were retrieved within one or two days after fish died, although one tag stopped recording data after ten days. The 2018 campaign was much less successful: two fish died one week after tagging, before any spawning acts were recorded; two fish lost their tags three and four days after tagging. The eleven remaining fish were radio tracked throughout the spawning season, until two exceptional floods (on June 7th and 16th) flushed them down to the estuary and the ocean where high water conductivity prevented further radio tracking, hence making tag retrieval impossible. Eventually, among the 25 tagged shad, only eight fully exploitable and one partially exploitable accelerograms could be collected. This sample of eight females represented half of the females that passed the Uxondoa weir in 2017, but the power of Spearman correlations to detect even a strong correlation of 0.5 between variables observed at the individual level was only 0.22. The minimal, median and maximal fork length and body mass of the eight females were 470, 510 and 550 mm, and 1320, 1635 and 1810 g.

According to their accelerograms, the eight female shad performed 7, 9, 12, 14, 14, 17, 24 and 26 spawning acts (mean=15.75). The total number of spawning acts performed by each female was correlated to none of the individual variables tested (Fig. 2).

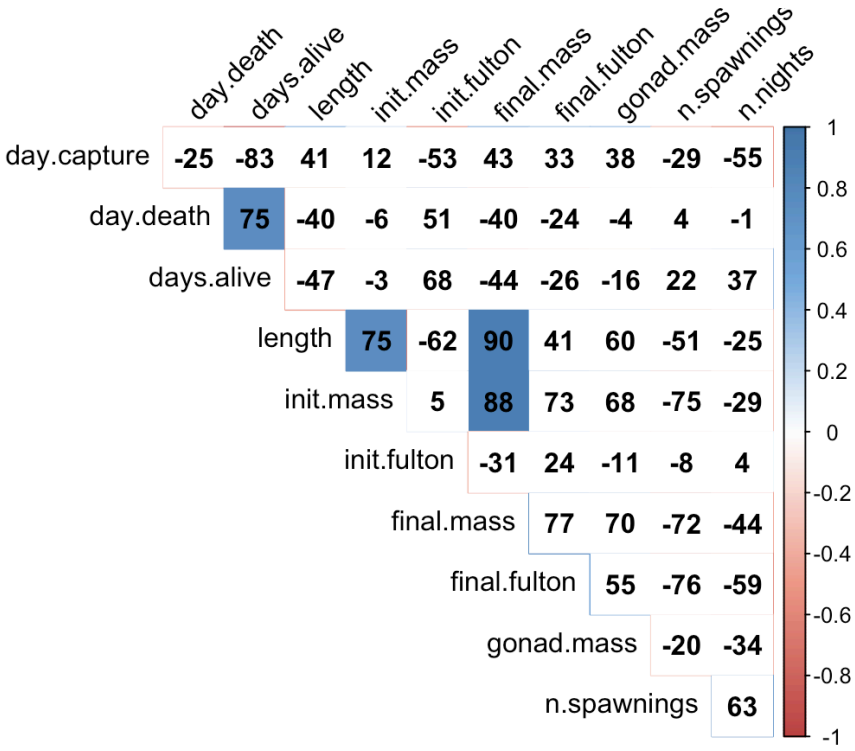

Figure 2. Spearman coefficient of correlation (expressed as percentage) between biometric and reproductive variables of female Allis shad. In order, day of capture, day of death, number of days between capture and death, body length, initial mass, initial Fulton coefficient of condition, final mass, final Fulton coefficient of condition, final gonad mass, number of spawning acts, number of nights with at least one spawning act.

For each female, spawning acts were distributed in three to six nights (mean=4.87) each separated by zero to eight nights (mean=3.55) without spawning acts, resulting in individual spawning seasons ranging from 14 to 24 nights (mean=18.12) from the first spawning act to the last (Fig. 3.A). The tagged females performed their first spawning act zero to eight days after tagging (mean=3). Only on eight occasions did a female perform a single spawning act during

a night, so the 137 remaining acts were performed in volleys. At the individual level, an active night comprised from two to eight acts (mean=3.23) performed in two to 84 minutes (mean=29.7). The mixed zero-inflated Poisson regression indicated that water temperature during the night had a positive effect on the probability that a female performed at least one spawning act (negative effect on the zero inflation; z=-1.95, p=0.05; probability of a spawning act estimated 0.18 at 18°C and 0.23 at 19°C) but no effect on the number of spawning acts in the volley (the Poisson component; z=-1.44, p=0.15). Cumulated over all the season, the temporal distribution of spawning acts within the night followed a Normal distribution, centred on 3AM, with 95% of spawning acts occurring between 0:30AM and 5:30AM. However, the permutation test on the hour of spawning acts indicated synchrony between acts performed by different females on the same night: the median time lag to the nearest act was one hour for observed data, which corresponds to the first percentile of simulated data (Fig. 3.B).

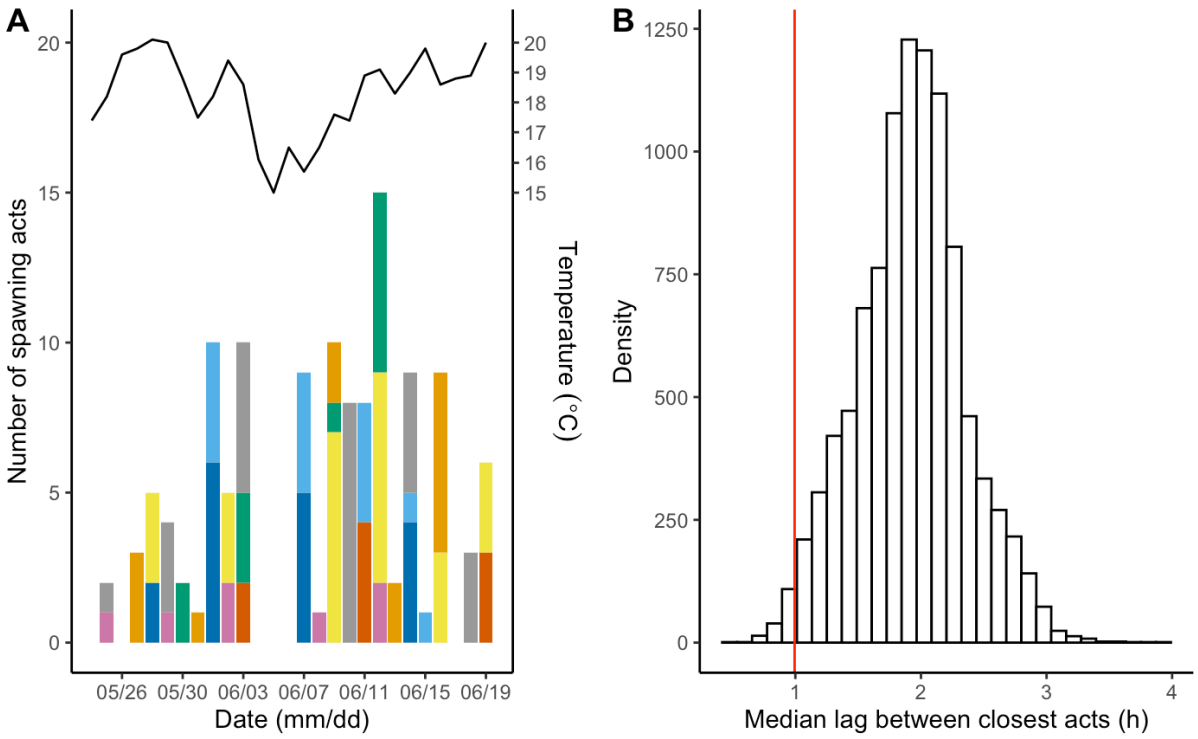

Figure 3. The temporal distribution of spawning acts by eight Allis shad females in the river Nivelle in spring 2017. A. Cumulated number of spawning acts for each night of the season.

Each colour corresponds to an individual. The line above the bar plot represents the average water temperature measured each night between 10PM and 7AM. B. Synchrony of spawning acts performed by different females within a night (only the first act of the night, for each female). The red vertical line represents the median time lag between nearest spawning acts for observed data. The histogram represents the same thing for 10 000 permutation of the hour of the acts.

Average tail beat frequency (TBF), temperature and depth were computed for 312 840 minutes across all individuals' spawning seasons (eight complete and one partial). Tail beat frequency ranged from 1.3 to 9.5 beats per second (mean=3.2), temperature ranged from 13.5 to 23.8°C (mean=18.3), and depth ranged from 0 to 400 cm (mean=186).

From equations (1) and (2), the estimated instantaneous rate of energy expenditure ranged from 0.09 to 0.89 $kJ.min^{-1}$ (mean=0.17), and total energy expenditure by each of the eight individuals from initial capture to death ranged from 4 395 to 8 361 kJ (mean=6 277; Fig. 4.A). The corresponding mass loss was estimated to range from 127 to 241 g (mean=181), representing from 9% to 17% of initial mass (mean=12%). The shad died 44 to 182 hours (mean=98.62) after their last spawning act. They had lost between 33% and 53% of their mass (mean=42%), and their ovaries weighed 25.9 to 141.5 g (mean=79.7). No correlation was found between mass loss and ovary mass (Spearman S=89.3; rho=-0.06; p=0.888). The predicted and observed mass lost during the season were positively correlated, (Spearman S=8.55; rho=0.9; p=0.002; Fig. 4.B), but the observed mass loss was on average 1.5 times more than predicted (479 g difference on average).

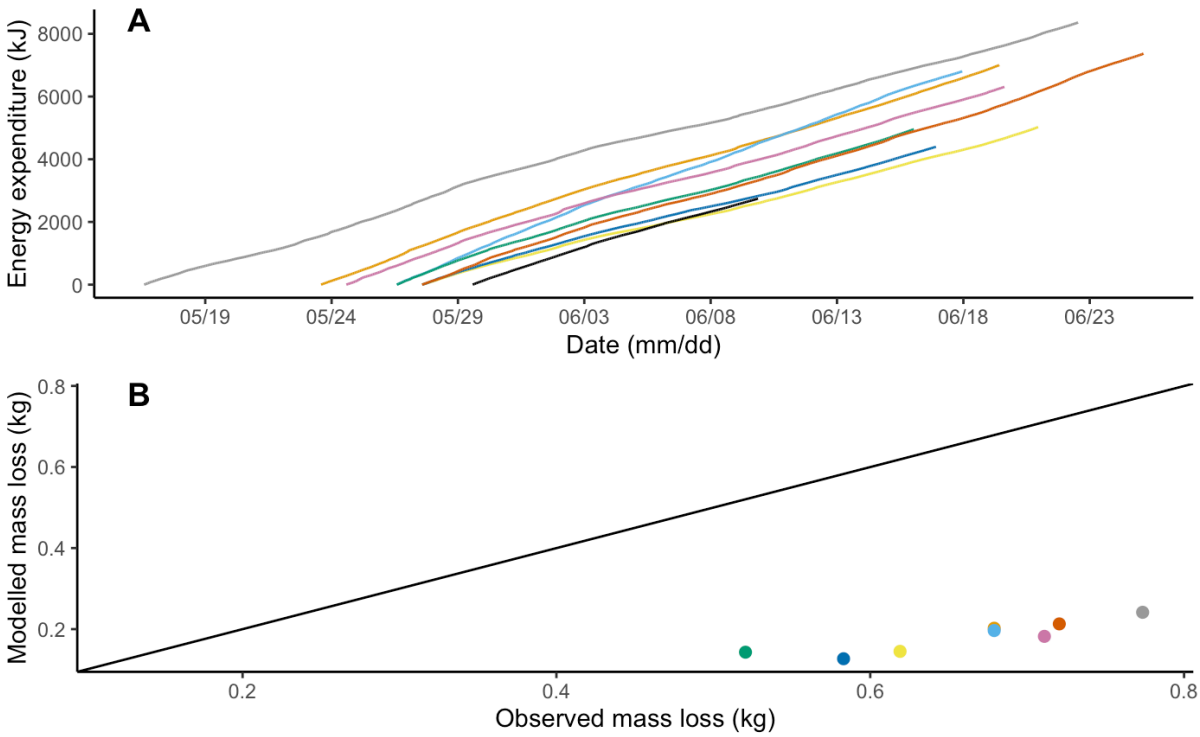

Figure 4. A. Energy expenditure over the spawning season for nine female Allis shad, estimated from temperature and tail beat frequency using equations (1) and (2). B. Observed mass loss and mass loss modelled with equations (1) and (2) over the spawning season. The straight line in B is the one on which points should lie if the modelled mass loss would fit the observations. Colours are as in Fig. 3, with black line in A for the individual whose tag stopped recording before the end of the experiment.

Aggregating TBF, temperature and pressure data over 8-hour periods (morning: 6AM-2PM, afternoon: 14PM-10PM, night: 10PM-6AM) produced 649 8-hour periods (Fig. 5). Shad stayed closer to the surface at night (163 cm) than during the morning and afternoon (200 cm) (LRT χ^2=238.9; p<0.0001; R^2_m=0.14; R^2_c=0.69), and experienced warmer temperature in the afternoon (18.5°C) than in the night (18.3°C) than in the morning (17.9°C) (LRT χ^2=15.8; p<0.0001; R^2_m=0.02; R^2_c=0.05). TBF was higher at night (3.24 beats/s) than in the afternoon (3.11 beats/s) than in the morning (3.06 beats/s) (LRT χ^2=26.8; p<0.0001) and was also 0.21 beats/s higher during the first nine periods (three days) just after tagging than afterwards (LRT

χ^2=37.6; p<0.0001; R^2_m=0.06; R^2_c=0.36 for the model including both effects). The estimated energy expenditure was the highest at night (83 kJ/8h), followed by afternoon (82 kJ/8h) and morning (77 kJ/8h) (LRT χ^2=24.8; p<0.0001; R^2_m=0.03; R^2_c=0.34). The mass of eggs remaining at death was not correlated to the energy expenditure cumulated across mornings (Spearman S=66; rho=0.21, p=0.619), afternoons (Spearman S=64; rho=24; p=0.582), nights (Spearman S=76; rho=0.09; p=0.84), or the whole season (Spearman S=64; rho=0.24; p=0.582).

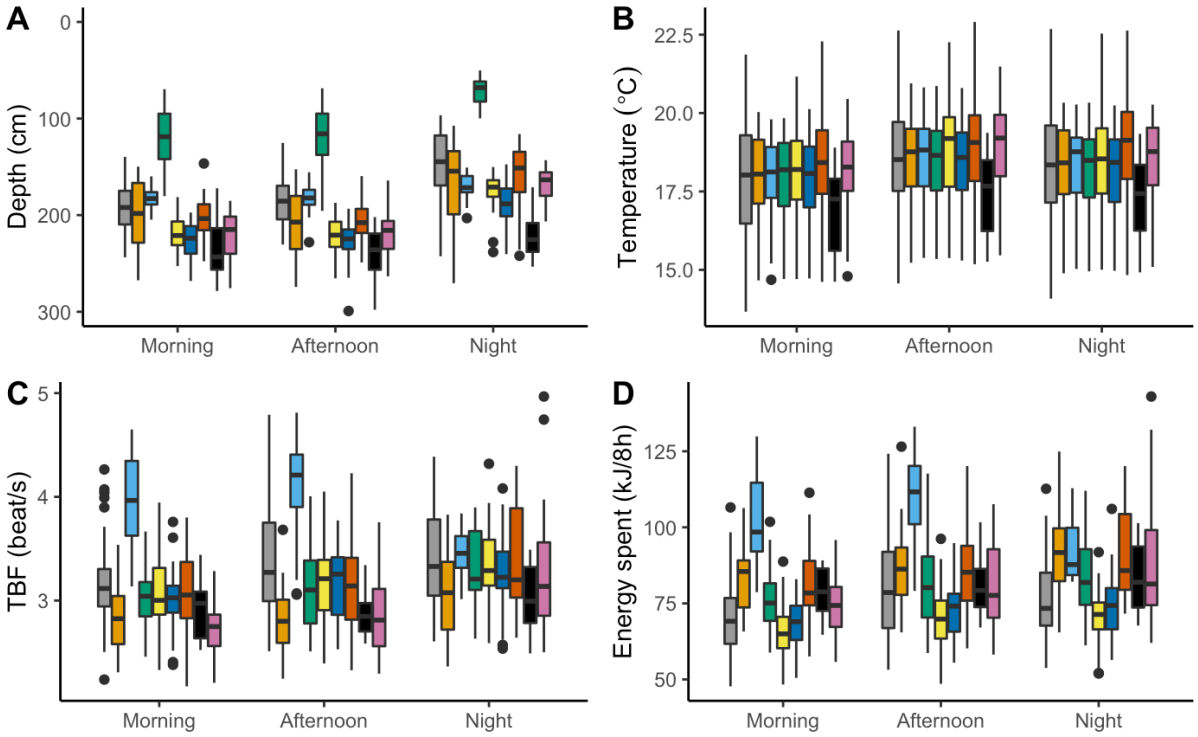

Figure 5. Depth (A), temperature (B), tail beat frequency (C) and estimated energy spent (D) by nine female allis shad during the morning (6AM:2PM), afternoon (2PM:10PM) and night (10PM:6AM) of their spawning season. Box plots show the distribution of the variables averaged (A, B, C) or cumulated (D) across 8-hour periods for each individual (colours as in Fig. 3, black for the individual whose tag stopped recording before the end of the experiment). In C, energy spent was computed from temperature and TBF using equations (1) and (2).

As expected, the θ angle between the x-axis of the accelerometer and the vertical plane was positively correlated to the individual's Fulton coefficient of condition (Pearson's r=0.63; p=0.006), although the effect seemed to be due to within-individual difference in condition and θ at the beginning and at the end of the season rather than inter-individual variability in condition and θ (Fig. 6.A). The θ angle globally decreased over time for all individuals and was negatively related to depth, resulting in occasional increases in θ during 8-hour periods when shad stayed closer to the surface (full model R^2_m=0.28; R^2_c=0.79; Fig. 6.B). The effect of time corresponded to a slope of -0.63 degree per day (LRT χ^2=518.4; p<0.001) and the effect of depth corresponded to a slope of -0.017 degree per cm (LRT χ^2=9.6; p=0.002). Contrary to our expectation, the difference of the θ angle between initial capture and death was not related to change in body condition between initial capture and final recapture (Spearman S=76, rho=0.09, p=0.84). The best mixed model to explain the shift in θ during a 8-hour period was the one with the moment (morning, afternoon or night) of the period as the independent factor (LRT χ^2=56.7; p<0.0001; R^2_m=0.08; R^2_c=0.08), followed by the null model including individual random effect only (ΔAICc=51), the model including estimated energy expenditure as the independent variable (ΔAICc=56), and the model including both temperature and TBF as independent variables (ΔAICc=58). According to the best model, the shift in θ was negative during mornings (mean ± standard deviation -1.25° ± 3.08), slightly negative during afternoons (-0.23° ± 2.36), and positive during the nights (0.89° ± 3.15).

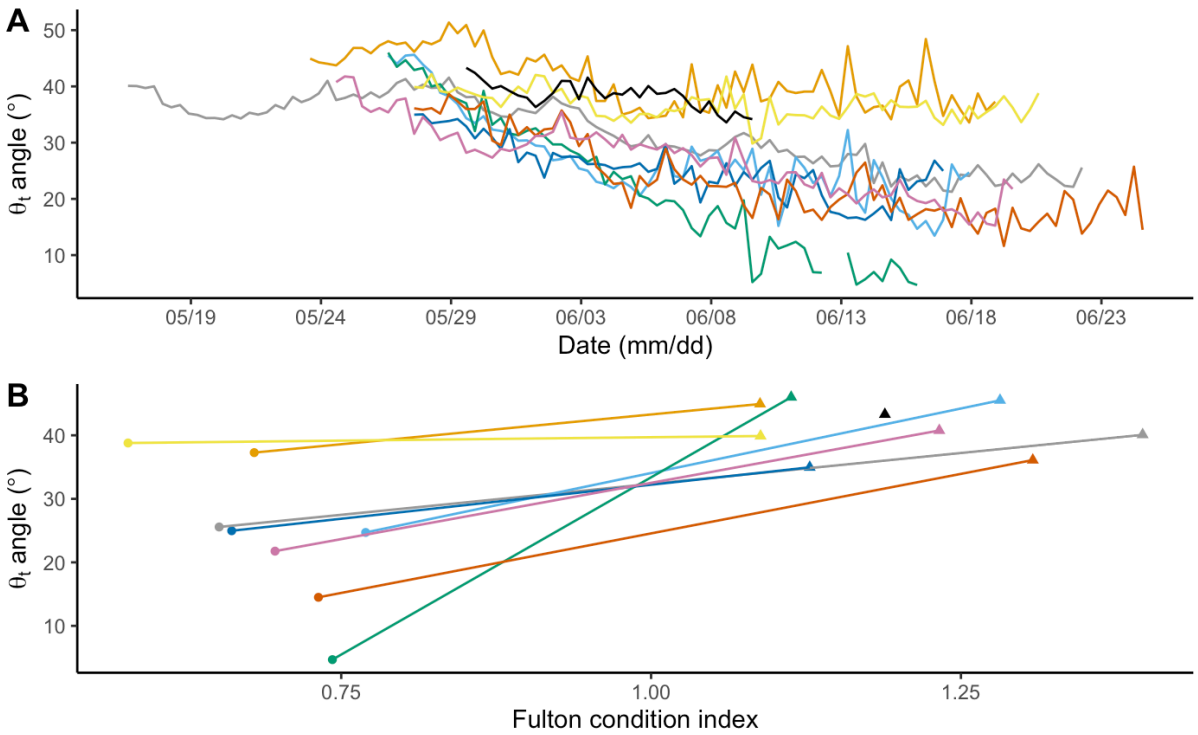

Figure 6. The θ_t angle between the x-axis of the accelerometer and the vertical plane as an indicator of fish body roundness A. Temporal evolution of θ computed each day along the spawning season for nine Allis shad. B. Relationship between Fulton coefficient of condition and θ_t angle at initial release (triangles) and at recapture after death (points). Each individual is represented with the same colour as in Fig. 3, and black is for the individual whose tag stopped recording before the end of the experiment.

Discussion

In this study, we used acceleration data to quantify the dynamics of spawning acts, energy expenditure and slimming of Allis shad females throughout their spawning season. The results indicate that the spawning schedule of shad females, although constrained by the serial maturation of oocyte batches, was also influenced by temperature and social factors: females had a higher probability to spawn during warmer nights, spawned repeatedly during most of their active nights and females that spawned on the same nights synchronized their spawning

acts with each other. Tail beat frequency and water temperature recorded by the loggers showed that energy expenditure was slightly higher during night time than during daytime, and may have been so high that shad died from energy exhaustion before having spawned all their eggs. Finally, the novel use of gravitational acceleration to monitor fish slimming, although perfectible, seems a promising method to monitor changes in animal condition in the field.

Dynamics of spawning acts and energy expenditure

The number of spawning acts performed by female Allis shad ranged from 7 to 26, with an average of 15.75. So far, the average individual number of spawning acts was indirectly estimated to be either five (Acolas et al., 2006) or 12 (Fatin and Dartiguelongue 1996) by counting the number of acts heard upstream a dam where all passing individuals were censused. Such method provides no estimate of interindividual variability. In a first attempt to work at the individual level, Acolas et al. (2004) marked three females and three males with acoustic tags, and based on the number of detections of the tags near the surface (assessed by the reception power by hydrophones immersed at different depth), estimated that zero, one and two acts were performed by the females and three, 38 and 60 acts by the males. Here, despite a small sample, we estimated a more representative distribution of the number of acts per individual, as their detection on accelerograms is certainly more reliable than the method used by Acolas et al. (2004). This distribution, as well as the timing of spawning acts, is crucial to build a model estimating the number of shad in a river from the acoustic survey of spawning acts, as it is routinely done in European rivers (e.g. Chanseau et al. 2004). Such a model, simulating shad spawning behaviour in an Approximate Bayesian Computation framework (ABC; Csilléry et al. 2010) is available in French here: https://ctentelier.shinyapps.io/alose_abc/. The number of acts per female could be correlated to none of the few biometric variables collected, but the very small sample implied a weak statistical power. Larger females, which have more eggs and

538 more energy, did not perform more spawning acts (a nonsignificant tendency towards negative
539 correlation was observed).

540 Beside oocyte maturation and temperature, the temporal distribution of spawning acts
541 was aggregated within and among females. While each female was active for most of the
542 population's spawning season, the individual spawning season was punctuated by three to six
543 nights of activity generally corresponding to volleys of two to eight acts performed in a few
544 tens of minutes, and separated by on average 3.5 nights of inactivity. The schedule of spawning
545 acts must be constrained by the fragmented maturation of oocytes (Cassou-Leins and Cassou-
546 Leins 1981; Olney et al. 2001), but also depended on temperature. Interestingly, while data
547 collected at the population level indicate that spawning activity increases with temperature
548 (Paumier et al. 2019), our data collected at the individual level showed that temperature
549 increased the probability that a female performed some acts during the night (the zero-inflation
550 component of the zero-inflated regression), but not the number of acts it performed (the count
551 component of the zero-inflated regression). In fact, two results suggest that the dynamics of
552 spawning acts within a night might be influenced by social factors. First, the temporal proximity
553 of acts performed by a given female in a given night in this study, and the high proportion of
554 acts performed without oocyte expulsion reported by Langkau et al. (2016) are reminiscent of
555 female trout's 'false orgasm' (Petersson 2001) or female lamprey's 'sham mating' (Yamazaki
556 and Koizumi 2017). For both of these species, it has been suggested that repeated spawning
557 simulations enable the female to exert mate choice, by both exhausting the sperm stock of an
558 unwanted courtier and signalling its mating activity to peripheral males. Second, spawning acts
559 of different females in a given night were more synchronous than expected from the hour of
560 spawning acts across all nights of the season. This suggests that a female which is ready to
561 spawn (mature batch of oocytes) in a propitious night (warm temperature) may trigger its
562 spawning acts when another female does so. Such fine scale synchrony in the mating activity

563 of different females may again affect sexual selection, reducing the environmental potential for
564 polygyny by making it difficult for the same male to monopolize several females at the same
565 time (Emlen and Oring 1977).

566 The end point in the spawning schedule of semelparous organisms is death, which
567 occurred in female shad two to seven days after their last spawning act, and before they laid all
568 their eggs, which suggests that energetic reserves were exhausted before egg stock. Combining
569 acceleration and temperature data collected in the field with equations parametrized in
570 laboratory experiments, we estimated that the energetic expenditure of spawning shad during
571 three weeks of spawning ranged from 4 395 to 8 361 kJ (mean=6 277). This is surprisingly of
572 the same order as female American shad, which entered the Connecticut river with a stock of
573 12 000 kJ, of which approximately 5 000 kJ were consumed along their 228-km and seven-
574 week long upstream migration in waters warming from 10 to 22°C (Leonard and McCormick
575 1999; but see next section for possible biases in our estimation). Extreme pre-spawning energy
576 expenditure caused by long migration, obstacle crossing or warm water can reduce the
577 reproductive lifespan of semelparous females and hinder their ability to spawn their full egg
578 stock (Hruska et al. 2011). While the spawning ground used by shad in our study is only 13 km
579 from the river mouth with only one obstacle to pass (Uxondoa, where we captured them), the
580 median daily temperature recorded in the Nivelle for May and June 2017 was 18.4°C, the
581 second warmest spring since the beginning of record in 1984, the maximum being 18.5°C in
582 1989, the minimum 14.6°C in 2013, and the median 16.9°C. According to our analysis of data
583 from Leonard et al. (1999; our equation 1), an increase in temperature from 16.9 to 18.4°C
584 would raise the energy expenditure by 8.3%, giving both a possible explanation for the inability
585 of shad to spawn all their eggs before they die and a hint of the impact of global warming on
586 the breeding performance of such species.

587 As expected from visual observations on spawning grounds, shads were more active at
588 night than during the day, and stayed deeper during daytime when water was warmer. Although
589 nocturnal spawning is usually interpreted as a strategy to decrease predation risk on spawners
590 or eggs (Robertson 1991), resting in deeper, hence fresher, water during the warm hours of the
591 day may also save energy for spawning at night. However, contrary to our predictions, the
592 individuals who spent less energy during mornings or afternoons and more during the night did
593 not have fewer residual eggs at death. Although our small sample size precludes conclusive
594 inferences, the continuous measurement of spawning activity and energy expenditure at the
595 individual level opens the door to the quantification and decomposition of interindividual
596 variation in the schedule of reproductive behaviour and energy management. Moreover,
597 coupling telemetric data on behaviour with additional fitness indicators such as offspring
598 production (egg sampling and genetic parentage analysis) could inform on the strength of
599 natural and sexual selection acting on these phenological strategies in the field (Tentelier et al.
600 2016).
601

602 ## Methodological considerations

603 According to calculated energy expenditure, the energetic model predicted that shad
604 should have lost on average 12% of their initial mass, which was much less than the observed
605 42% loss. Of course, the energetic model did not account for egg expulsion, which must
606 represent a large proportion of mass loss, given that ovaries can represent up to 15% of somatic
607 mass at the onset of the spawning season (Cassou-Leins and Cassou-Leins 1981; Taverny
608 1991). Moreover, the equations used to convert TBF and temperature to energy expenditure
609 and mass loss were not parametrized with data obtained on *A. alosa* but on *A. sapidissima*
610 (Castro-Santos & Letcher, 2010; Leonard et al., 1999; Leonard & McCormick, 1999) which is
611 the species most closely related to *A. alosa* for which such reliable information exist. Although

American shad and Allis shad have the same morphology and ecology, some elements suggest that results on American shad could not exactly apply to our study on Allis shad, and that our estimates of energy expenditure should be taken cautiously. First, although the range of temperatures used by Leonard et al. (1999) were similar to the temperatures encountered by shad in our study, TBF of Allis shad in the field exceeded the fastest swim tested by Leonard et al. (1999). In particular, the brief bouts of very high TBF which correspond to spawning acts may represent anaerobic efforts, which are sustained by white muscle rather than red muscle and are more costly than the aerobic effort observed by Leonard et al. (1999). Given the difference in mechano-chemical efficiency (ratio of mechanical power output to chemical energy consumed) between red and white muscles, a different equation should be calibrated for each type of effort (Gleiss et al. 2011). The volleys of spawning acts performed by females in a few tens of minutes could even lead to sexual selection of traits affecting the recovery after sprint (Kieffer 2000). Second, the relationship linking swim speed to oxygen demand (MO_2) varies between species, even closely related, and American shad seems to have a particularly high metabolism compared to other clupeids (Leonard et al. 1999). This would have led to an overestimation of energy costs for *A. alosa*. Third, the relative contribution of lipids and proteins as metabolic fuel may differ between the iteroparous American shad and the semelparous Allis shad. Indeed, as migratory iteroparous fishes have to conserve proteins, especially in the red muscle, for their downstream migration, semelparous species can exhaust their protein stock to complete spawning (Schultz 1999). Also, Leonard & McCormick (1999) measured the relative expenditure of lipids and proteins in *migrating* American shad, while we monitored *spawning* Allis shad. It has been shown that most anadromous fishes catabolise proteins only when lipid reserves have been exhausted, in a way that lipids mainly fuel migration while proteins fuel spawning (Idler and Bitners 1958; Beamish et al. 1979; Jonsson et al. 1997; Hendry and Berg 1999). Given that proteins have a lower energy density than lipids,

637 the surprising high energy consumption and the low mass loss predicted by the energetic model
638 may be explained by spawning Allis shad relying more on proteins than on lipids. All these
639 caveats could be avoided by laboratory calibration of the equations relating energy expenditure
640 to tail beat frequency and temperature on the same species, at the same stage of energy reserves,
641 bearing the same tags and performing the same behaviours as in the field.

642 While the presence of the radio tag and the accelerometer may have imposed an
643 energetic cost on shad due to additional mass (less than 2% of initial fish mass) and drag, several
644 indicators suggest that our tagging method did not impact shad behaviour as heavily than the
645 commonly gastric implants which result in high mortality rate or long post-tagging downstream
646 movements (Steinbach et al. 1986; Verdeyroux et al. 2015; Tétard et al. 2016). Such
647 downstream movements were only observed in 2018, after exceptional floods which have
648 probably also make untagged shad drift downstream, especially after the spawning season.
649 Although the dead individuals we retrieved in 2017 showed clear depigmentation, neither
650 severe abrasion nor fungal proliferation was observed, even after one month in water at 18° C.
651 Moreover, the eight females for which complete accelerograms were retrieved all spawned,
652 three of them spawned the night directly following tagging, and the median of 14 spawning acts
653 was above the five to twelve acts per individuals estimated by Acolas *et al.* (2006) and Fatin &
654 Dartiguelongue (1996). However, shad may have suffered post-tagging stress, as indicated by
655 the higher tail beat frequency (TBF) during the three days following tagging that during the
656 remainder of the spawning season, consistent with the increased activity of Atlantic salmon
657 during the three days after tagging (Føre et al. 2020). On the other hand, a higher TBF just after
658 tagging may be due to the fish finishing their upstream migration, before settling near spawning
659 grounds (unpublished radio tracking data). This moderate negative impact suggests that
660 external tagging under the dorsal fin, provided fish are continually kept immerged and rapidly
661 handled, is a suitable tagging technique for Allis shad (Jepsen et al. 2015; Breine et al. 2017).

662 Although the swimming behaviour did not seem to be strongly impaired, the additional weight
663 or drag force caused by the tag may have increased the energy required to perform this
664 behaviour (Jepsen et al. 2015). In this case, the energy expenditure of tagged fish computed
665 from equations derived from swim tunnel experiments performed on untagged fish would be
666 underestimated. To develop the telemetric measurement of realistic energy expenditure,
667 attention should be paid to both designing tags that do not impose too much additional energetic
668 costs on individuals and estimating these additional costs.

669 On top of the estimation of energetic costs from dynamic acceleration, the continuous
670 estimation of body roundness from static acceleration is a promising yet perfectible application.
671 Gravitational acceleration is commonly used to infer the posture of the animal, assuming that
672 the position of the accelerometer on the animal is constant (Brown et al. 2013). Here, assuming
673 that shad stayed upright for most of the time, gravitational acceleration was used as an indicator
674 of change in body shape. In particular, we hypothesized that the angle θ between the x axis of
675 the accelerometer and the vertical plane may indicate body roundness. For all individuals, θ
676 was higher at the beginning of the season than at the end, when the fish had thinned, and
677 globally decreased along the spawning season. The accelerometer was attached under the dorsal
678 fin, where the cross-section is the broadest, which probably maximized the sensitivity of
679 acceleration data to fish slimming. Furthermore, shad mainly store energy for migration and
680 spawning as subdermal fat and interstitial fat in the white muscle (Leonard and McCormick
681 1999), whereas the limited consumption of visceral and liver fat may not have affected θ.
682 However, interindividual variability in θ was not correlated to interindividual variability in
683 body condition, and the shift in θ was not correlated to individual mass loss during the spawning
684 season. This could be due to interindividual differences in the exact position of the
685 accelerometers on the fish, or in the relationship between body condition and roundness. Indeed,
686 mass loss due to gamete expulsion was probably undetectable by the accelerometer attached to

the back of the fish. Given that ovaries can represent up to 15% of a shad mass at arrival on spawning grounds (Cassou-Leins and Cassou-Leins 1981; Taverny 1991), a significant loss of mass was probably not reflected in the rotation of the accelerometer across the spawning season. In fact, shift of θ across eight hour periods increased with neither TBF, temperature, nor estimated energy expenditure, contrary to what was expected from the relationship linking TBF and temperature to energy consumption in American shad (Leonard et al. 1999). This lack of resolution may be due to the way tags were attached. In particular, while the attachment wires were tightened during the tagging procedure, fish slimming loosened them so the accelerometer must have jiggled more and more as fish thinned, thereby increasing the noise in acceleration data. Given all these results and limits, using the angle of the accelerometer to quantitatively track change in mass or body roundness will certainly require further tuning, such as laboratory experiment with repeated weighing and image analysis of the fish's cross-section, and drastic standardization of attachment procedure, but we consider it a promising method to monitor individual condition in the field. On top of slimming, θ was linked to depth, and increased during some periods when the fish stayed closer to the surface, in particular during nights. This was probably due to the inflation of the swim bladder, which represents around 8% of the volume of the fish, and inflates as the fish stays closer to the surface (Alexander 1966). Although here, swim bladder inflation introduced additional variation in our monitoring of fish slimming, it could also be the process of interest in some field studies, for example to untangle the contribution of swim bladder inflation and active swimming in the vertical migration of pelagic fishes (e.g. Pelster 2015). This illustrates the potentially broad application of our acceleration-based approached, which, once refined, could be used to detect the many ecologically or behaviourally relevant changes in animal shape beyond slimming due to energy consumption, such as parturition, massive food intake in large predators (Cuyper et al. 2019), inflammatory swelling (Duncan et al. 2016), or inflation as a courtship or defence behaviour

(Wainwright and Turingan 1997). Combined with dynamic acceleration, such data could be used to test whether these changes in shape are associated to global activity or to the expression of specific behaviours.

Acknowledgements

We thank B. Liquet, F. Luthon, B. Larroque and E. Bouix for their help in the initial exploration of data, and J. Leonard and T. Castro-Santos for sharing their data on American shad. This study was financed by the Adour-Garonne Water Agency, and the French region Nouvelle Aquitaine.

Conflict of interest disclosure

The authors of this article declare that they have no financial conflict of interest with the content of this article.

References

Acolas M, Veron V, Jourdan H, Begout M, Sabatie M, Bagliniere J l. 2006. Upstream migration and reproductive patterns of a population of allis shad in a small river (L'Aulne, Brittany, France). doi:DOI:10.1016/j.icesjms.2005.05.022.

Acolas ML, Anras MLB, Véron V, Jourdan H, Sabatié MR, Baglinière JL. 2004. An assessment of the upstream migration and reproductive behaviour of allis shad (*Alosa alosa* L.) using acoustic tracking. ICES J Mar Sci. 61(8):1291–1304. doi:10.1016/j.icesjms.2004.07.023.

Alexander RM. 1966. Physical aspects of swimbladder function. Biological Reviews. 41(1):141–176. doi:10.1111/j.1469-185X.1966.tb01542.x.

Anderson SS, Fedak MA. 1985. Grey seal males: energetic and behavioural links between size and sexual success. Animal Behaviour. 33(3):829–838. doi:10.1016/S0003-3472(85)80017-8.

Baglinière J-L, Elie P. 2000. Les Aloses (*Alosa alosa* et *Alosa fallax* spp.): écobiologie et variabilité des populations. Editions Quae.

Baglinière J-L, Sabatié M-R, Rochard E, Alexandrino P, Aprahamian MW. 2003. The Allis shad *Alosa alosa*: Biology, ecology, range and status of populations. In: Biology, Status and Conservation of the World's Shads. American Fisheries Society. p. 85–102.

Barton K. 2009. MuMIn: Multimodel inference. https://cran.r-project.org/web/packages/MuMIn/index.html.

Bates D, Maechler M, Bolker B, Walker S. 2014. lme4: Linear mixed-effects models using Eigen and S4.

Beamish FWH, Potter IC, Thomas E. 1979. Proximate composition of the adult anadromous sea lamprey, *Petromyzon marinus*, in relation to feeding, migration and reproduction. Journal of Animal Ecology. 48(1):1–19. doi:10.2307/4096.

Bengen GSH. 1992. Suivi de la maturation gonadique des aloses, *Alosa alosa* L. lors de leur migration en Garonne. PhD thesis, Toulouse, France: Institut national polytechnique.

Bonnet X, Bradshaw D, Shine R. 1998. Capital versus income breeding: an ectothermic perspective. Oikos. 83(2):333–342.

Borgia G. 1985. Bower quality, number of decorations and mating success of male satin bowerbirds (*Ptilonorhynchus violaceus*): an experimental analysis. Animal Behaviour. 33(1):266–271. doi:10.1016/S0003-3472(85)80140-8.

Breine J, Pauwels IS, Verhelst P, Vandamme L, Baeyens R, Reubens J, Coeck J. 2017. Successful external acoustic tagging of twaite shad *Alosa fallax* (Lacépède 1803). Fisheries Research. 191(Supplement C):36–40. doi:10.1016/j.fishres.2017.03.003.

Brett JR, Groves TDD. 1979. Physiological energetics. In: Hoar WS, Randall DJ, Brett JR, editors. Bioenergetics and growth. Vol. 8. Academic Press. New York. (Fish physiology). p. 279–352.

Broell F, Taggart CT. 2015. Scaling in free-swimming fish and implications for measuring size-at-time in the wild. PLoS One. 10(12). doi:10.1371/journal.pone.0144875.

Brooks ME, Kristensen K, Benthem KJ van, Magnusson A, Berg CW, Nielsen A, Skaug HJ, Mächler M, Bolker BM. 2017. glmmTMB balances speed and flexibility among packages for zero-inflated generalized linear mixed modeling. The R Journal. 9(2):378–400.

Brown DD, Kays R, Wikelski M, Wilson R, Klimley AP. 2013. Observing the unwatchable through acceleration logging of animal behavior. Animal Biotelemetry. 1(1):1–16. doi:10.1186/2050-3385-1-20.

Brownscombe JW, Lennox RJ, Danylchuk AJ, Cooke SJ. 2018. Estimating fish swimming metrics and metabolic rates with accelerometers: the influence of sampling frequency. J Fish Biol. 93(2):207–214. doi:10.1111/jfb.13652.

Casas J, Pincebourde S, Mandon N, Vannier F, Poujol R, Giron D. 2005. Lifetime nutrient

dynamics reveal simultaneous capital and income breeding in a parasitiod. Ecology. 86(3):545–554. doi:10.1890/04-0812.

Cassou-Leins F, Cassou-Leins J-J. 1981. Recherches sur la biologie et l'halieutique des migrateurs de la Garonne et principalement l'alose : *Alosa alosa*. PhD thesis, Institut National Polytechnique de Toulouse.

Castro-Santos T, Letcher BH. 2010. Modeling migratory energetics of Connecticut River American shad (*Alosa sapidissima*): implications for the conservation of an iteroparous anadromous fish. Can J Fish Aquat Sci. 67(5):806–830. doi:10.1139/F10-026.

Chanseau M, Castelnaud G, Carry L, Martin-Vandembulcke D, Belaud A. 2004. Essai d'évaluation du stock de géniteurs d'alose *Alosa alosa* du bassin versant Gironde-Garonne-Dordogne sur la période 1987-2001 et comparaison de différents indicateurs d'abondance. Bulletin Français de la Pêche et de la Pisciculture.(374):1–19. doi:10.1051/kmae:2004023.

Collins PM, Halsey LG, Arnould JPY, Shaw PJA, Dodd S, Green JA. 2016. Energetic consequences of time-activity budgets for a breeding seabird. J Zool. 300(3):153–162. doi:10.1111/jzo.12370.

Craig JF, Kenley MJ, Talling JF. 1978. Comparative estimations of the energy content of fish tissue from bomb calorimetry, wet oxidation and proximate analysis. Freshwater Biology. 8(6):585–590. doi:10.1111/j.1365-2427.1978.tb01480.x.

Csilléry K, Blum MGB, Gaggiotti OE, François O. 2010. Approximate Bayesian Computation (ABC) in practice. Trends in Ecology & Evolution. 25(7):410–418. doi:10.1016/j.tree.2010.04.001.

Cuyper AD, Clauss M, Carbone C, Codron D, Cools A, Hesta M, Janssens GPJ. 2019. Predator size and prey size–gut capacity ratios determine kill frequency and carcass production in terrestrial carnivorous mammals. Oikos. 128(1):13–22.

798 doi:10.1111/oik.05488.

799 Duncan AE, Torgerson-White LL, Allard SM, Schneider T. 2016. An evaluation of infrared
800 thermography for detection of bumblefoot (pododermatitis) in penguins. J Zoo Wildl
801 Med. 47(2):474–485. doi:10.1638/2015-0199.1.

802 ECP. 2018. Ecology and Fish Population Biology Facility.
803 doi:10.15454/1.5572402068944548E12.

804 Emlen ST, Oring LW. 1977. Ecology, sexual selection, and the evolution of mating systems.
805 Science. 197(4300):215–223. doi:10.1126/science.327542.

806 Fatin D, Dartiguelongue J. 1996. Etude préliminaire de la reproduction des aloses en 1995
807 entre Tuilières et Mauzac sur la Dordogne.

808 Føre M, Svendsen E, Økland F, Gräns A, Alfredsen JA, Finstad B, Hedger R, Uglem I. 2020.
809 Heart rate and swimming activity as indicators of post-surgical recovery time of Atlantic
810 salmon (*Salmo salar*). doi:10.21203/rs.3.rs-23506/v1.

811 Fürtbauer I, Mundry R, Heistermann M, Schülke O, Ostner J. 2011. You mate, I mate:
812 Macaque females synchronize sex not cycles. PLOS ONE. 6(10):e26144.
813 doi:10.1371/journal.pone.0026144.

814 Gauthey Z, Freychet M, Manicki A, Herman A, Lepais O, Panserat S, Elosegi A, Tentelier C,
815 Labonne J. 2015. The concentration of plasma metabolites varies throughout
816 reproduction and affects offspring number in wild brown trout (*Salmo trutta*).
817 Comparative Biochemistry and Physiology Part A: Molecular & Integrative Physiology.
818 184:90–96. doi:10.1016/j.cbpa.2015.01.025.

819 Gleiss AC, Wilson RP, Shepard ELC. 2011. Making overall dynamic body acceleration work:
820 on the theory of acceleration as a proxy for energy expenditure. Methods in Ecology and
821 Evolution. 2(1):23–33. doi:10.1111/j.2041-210X.2010.00057.x.

822 Gochfeld M. 1980. Mechanisms and adaptive value of reproductive synchrony in colonial

seabirds. In: Burger J, Olla BL, Winn HE, editors. Behavior of marine animals: Current perspectives in research. Marine birds. Boston, MA: Springer US. p. 207–270.

Groscolas R, Viera V, Guerin N, Handrich Y, Côté SD. 2010. Heart rate as a predictor of energy expenditure in undisturbed fasting and incubating penguins. Journal of Experimental Biology. 213(1):153–160. doi:10.1242/jeb.033720.

Heimpel GE, Rosenheim JA. 1998. Egg limitation in parasitoids: A review of the evidence and a case study. Biological Control. 11(2):160–168. doi:10.1006/bcon.1997.0587.

Hendry AP, Beall E. 2004. Energy use in spawning Atlantic salmon. Ecology of Freshwater Fish. 13(3):185–196. doi:10.1111/j.1600-0633.2004.00045.x.

Hendry AP, Berg OK. 1999. Secondary sexual characters, energy use, senescence, and the cost of reproduction in sockeye salmon. Can J Zool. 77(11):1663–1675. doi:10.1139/z99-158.

Hicks O, Burthe S, Daunt F, Butler A, Bishop C, Green JA. 2017. Validating accelerometry estimates of energy expenditure across behaviours using heart rate data in a free-living seabird. Journal of Experimental Biology.:jeb.152710. doi:10.1242/jeb.152710.

Hruska KA, Hinch SG, Patterson DA, Healey MC. 2011. Egg retention in relation to arrival timing and reproductive longevity in female sockeye salmon (*Oncorhynchus nerka*). Can J Fish Aquat Sci. 68(2):250–259. doi:10.1139/F10-153.

Hughes PW. 2017. Between semelparity and iteroparity: Empirical evidence for a continuum of modes of parity. Ecol Evol. 7(20):8232–8261. doi:10.1002/ece3.3341.

Idler DR, Bitners I. 1958. Biochemical studies on sockeye salmon during spawning migration: Ii. Cholesterol, fat, protein, and water in the flesh of standard fish. Can J Biochem Physiol. 36(8):793–798. doi:10.1139/o58-084.

Ims RA. 1990. The ecology and evolution of reproductive synchrony. Trends in Ecology & Evolution. 5(5):135–140.

848 Jepsen N, Thorstad EB, Havn T, Lucas MC. 2015. The use of external electronic tags on fish:
849 an evaluation of tag retention and tagging effects. Animal Biotelemetry. 3(1):49.
850 doi:10.1186/s40317-015-0086-z.
851 Jonsson N, Jonsson B, Hansen LP. 1997. Changes in proximate composition and estimates of
852 energetic costs during upstream migration and spawning in Atlantic salmon *Salmo salar*.
853 Journal of Animal Ecology. 66(3):425–436. doi:10.2307/5987.
854 Jovani R, Grimm V. 2008. Breeding synchrony in colonial birds: from local stress to global
855 harmony. Proceedings of the Royal Society B: Biological Sciences. 275(1642):1557–
856 1564. doi:10.1098/rspb.2008.0125.
857 Kawabe R, Kawano T, Nakano N, Yamashita N, Hiraishi T, Naito Y. 2003. Simultaneous
858 measurement of swimming speed and tail beat activity of free-swimming rainbow trout
859 *Oncorhynchus mykiss* using an acceleration data-logger. Fisheries science. 69(5):959–
860 965. doi:10.1046/j.1444-2906.2003.00713.x.
861 Kieffer JD. 2000. Limits to exhaustive exercise in fish. Comp Biochem Physiol, Part A Mol
862 Integr Physiol. 126(2):161–179.
863 Kirkendall LR, Stenseth NChr. 1985. On defining 'breeding once'. The American Naturalist.
864 125(2):189–204.
865 Koizumi I, Shimatani IK. 2016. Socially induced reproductive synchrony in a salmonid: an
866 approximate Bayesian computation approach. Behav Ecol. 27(5):1386–1396.
867 doi:10.1093/beheco/arw056.
868 Langkau MC, Clavé D, Schmidt MB, Borcherding J. 2016. Spawning behaviour of Allis shad
869 *Alosa alosa*: new insights based on imaging sonar data. J Fish Biol. 88(6):2263–2274.
870 doi:10.1111/jfb.12978.
871 Leonard JBK, McCormick SD. 1999. Effects of migration distance on whole-body and tissue-
872 specific energy use in American shad (*Alosa sapidissima)*. Can J Fish Aquat Sci.

873 56(7):1159–1171. doi:10.1139/f99-041.

874 Leonard JBK, Norieka JF, Kynard B, McCormick SD. 1999. Metabolic rates in an
875 anadromous clupeid, the American shad (*Alosa sapidissima*). J Comp Physiol B. 169(4–
876 5):287–295. doi:10.1007/s003600050223.

877 Mennesson-Boisneau C, Boisneau P. 1990. Migration, répartition, reproduction,
878 caractéristiques biologiques et taxonomie des aloses (*Alosa* sp) dans le bassin de la Loire.
879 PhD thesis, Université de Rennes et Paris XII.

880 Nagy KA, Girard IA, Brown TK. 1999. Energetics of free-ranging mammals, reptiles, and
881 birds. Annu Rev Nutr. 19:247–277. doi:10.1146/annurev.nutr.19.1.247.

882 Olney JE, Denny SC, Hoenig JM. 2001. Criteria for determining maturity stage in female
883 American shad, *Alosa sapidissima*, and a proposed reproductive cycle. Bull Fr Pêche
884 Piscic.(362–363):881–901. doi:10.1051/kmae:2001025.

885 Paumier A, Drouineau H, Carry L, Nachón DJ, Lambert P. 2019. A field-based definition of
886 the thermal preference during spawning for allis shad populations (*Alosa alosa*).
887 Environmental Biology of Fishes. 102(6):845–855. doi:10.1007/s10641-019-00874-7.

888 Pelster B. 2015. Swimbladder function and the spawning migration of the European eel
889 *Anguilla anguilla*. Front Physiol. 5. doi:10.3389/fphys.2014.00486.

890 Petersson E. 2001. 'False orgasm' in female brown trout: trick or treat? Animal Behaviour.
891 61(2):497–501. doi:10.1006/anbe.2000.1585.

892 Pianka ER. 1976. Natural selection of optimal reproductive tactics. American Zoologist.
893 16(4):775–784.

894 R Development Core Team. 2008. R: A language and environment for statistical computing.
895 R Foundation for Statistical Computing, Vienna, Austria. http://www.R-project.org.

896 Rands SA, Houston AI, Cuthill IC. 2006. Measurement of mass change in breeding birds: A
897 bibliography and discussion of measurement techniques. Ringing & Migration. 23(1):1–

5. doi:10.1080/03078698.2006.9674337.

Robertson DR. 1991. The role of adult biology in the timing of spawning of tropical reef fishes. In: Sale PF, editor. The Ecology of fishes on coral reefs. San Diego: Academic Press. p. 356–386. http://www.sciencedirect.com/science/article/pii/B9780080925516500180.

Roff D. 1993. Evolution of life histories: Theory and analysis. Springer Science & Business Media.

Schultz DL. 1999. Comparison of lipid levels during spawning in annual and perennial darters of the subgenus *Boleosoma*, *Etheostoma perlongum*, and *Etheostoma olmstedi*. Copeia. 1999(4):906–916. doi:10.2307/1447966.

Stearns SC. 1992. The evolution of life histories. OUP Oxford.

Steinbach P, Gueneau P, Autuoro A, Broussard D. 1986. Radio-pistage de grandes aloses adultes en Loire. Bulletin Français de la Pêche et de la Pisciculture.(302):106–117. doi:10.1051/kmae:1986007.

Taverny C. 1991. Contribution à la connaissance de la dynamique des populations d'aloses : *Alosa Alosa* et *Alosa Fallax* dans le système fluvio-estuarien de la Gironde : pêche, biologie et écologie : étude particulière de la devalaison et de l'impact des activités humaines. PhD thesis, Université de Bordeaux 1.

Tentelier C, Larranaga N, Lepais O, Manicki A, Rives J, Lange F. 2016. Space use and its effects on reproductive success of anadromous Atlantic salmon. Canadian Journal of Fisheries and Aquatic Sciences. 73(10):1461–1471. doi:10.1139/cjfas-2015-0518.

Tétard S, Feunteun E, Bultel E, Gadais R, Bégout M-L, Trancart T, Lasne E. 2016. Poor oxic conditions in a large estuary reduce connectivity from marine to freshwater habitats of a diadromous fish. Estuarine, Coastal and Shelf Science. 169:216–226. doi:10.1016/j.ecss.2015.12.010.

Tsuda Y, Kawabe R, Tanaka H, Mitsunaga Y, Hiraishi T, Yamamoto K, Nashimoto K. 2006. Monitoring the spawning behaviour of chum salmon with an acceleration data logger. Ecology of Freshwater Fish. 15(3):264–274. doi:10.1111/j.1600-0633.2006.00147.x.

Verdeyroux P, Guerri O, Chanseau M, Cazeaux J, Fauvel F, Bogun F, Desmoulin A, Tarrene C, Nicole T, Dubois A, et al. 2015. Radio-telemetry study of the Allis shad (*Alosa alosa*) migration at Bergerac and Tuilières along the Dordigne river and at Golfech along the Garonne river from 2011 to 2014. Epidor.

Wainwright PC, Turingan RG. 1997. Evolution of pufferfish inflation behavior. Evolution. 51(2):506–518. doi:10.1111/j.1558-5646.1997.tb02438.x.

Wilson RP, Börger L, Holton MD, Scantlebury DM, Gómez-Laich A, Quintana F, Rosell F, Graf PM, Williams H, Gunner R, et al. 2019. Estimates for energy expenditure in free-living animals using acceleration proxies: A reappraisal. Journal of Animal Ecology. 89(1):161–172. doi:10.1111/1365-2656.13040.

Wilson RP, White CR, Quintana F, Halsey LG, Liebsch N, Martin GR, Butler PJ. 2006. Moving towards acceleration for estimates of activity-specific metabolic rate in free-living animals: the case of the cormorant. J Anim Ecol. 75(5):1081–1090. doi:10.1111/j.1365-2656.2006.01127.x.

Yamazaki C, Koizumi I. 2017. High frequency of mating without egg release in highly promiscuous nonparasitic lamprey *Lethenteron kessleri*. J Ethol. 35(2):237–243. doi:10.1007/s10164-017-0505-0.